

A TWO-SCALE MULTIPLE SCATTERING PROBLEM*

KAI HUANG[†] AND PEIJUN LI[‡]

Abstract. Consider the scattering problem of a time-harmonic plane wave incident on a heterogeneous medium consisting of isotropic point (small scale) scatterers and an extended (wavelength comparable) obstacle scatterer in three-dimensional space. To compute the scattered field from the interaction between the incident wave and the point scatterers only, the Foldy–Lax method provides an effective approach, while boundary integral equation methods play an important role for solving the scattering problem solely involving an extended obstacle scatterer. It is a challenging two-scale multiple scattering problem when both the point scatterers and the extended obstacle are present. In this paper, a generalized Foldy–Lax method is developed to fully take account of the multiple scattering in the heterogeneous medium. The method is viewed from two different formulations: the series solution and the integral equation. The series solution formulation is shown as an efficient iterative scheme to the integral equation formulation. The convergence of the scattered fields and the far-field patterns from the series solution formulation are characterized in terms of scattering coefficients. Numerical experiments are presented to show the agreement and the effectiveness of the proposed two approaches.

Key words. Foldy–Lax formulation, isotropic point scatterers, obstacle scattering problems, Helmholtz equation

AMS subject classifications. 78A45, 78M15, 65N12

DOI. 10.1137/090771090

1. Introduction. Scattering problems are concerned with the effect an inhomogeneous medium has on an incident wave [4]. In particular, if the total field is viewed as the sum of the incident field and the scattered field, the direct scattering problem is to determine the scattered field from the knowledge of the incident field, the scatterers, and the differential equation governing the wave motion. Scattering problems are basic in many scientific areas such as radar and sonar (e.g., submarine detection), geophysical exploration (e.g., oil and gas exploration), and medical imaging (e.g., breast cancer detection). Multiple scattering, which is interesting and challenging, refers to the interaction of the wave fields with two or more obstacles with possible different scales [11]. This work is devoted to a two-scale multiple acoustic wave scattering problem of a time-harmonic plane wave incident on a heterogeneous medium consisting of isotropic point scatterers and an extended obstacle scatterer. “Isotropic point” refers that the scale of the scatterer is much smaller than the wavelength of the incident field so that the scatterer can be represented by a source point within it; “extended” means that the scale of the obstacle scatterer is comparable with the wavelength of the incident field.

The Foldy–Lax method is concerned with the multiple scattering of scalar waves by a distribution of small isotropic scatterers [7, 10]. This self-consistent method assumes that a wave is emitted by each scatterer of an amount and directionality determined by the radiation incident on that scatterer (the effective field). The latter

*Received by the editors September 15, 2009; accepted for publication (in revised form) June 18, 2010; published electronically August 24, 2010.

<http://www.siam.org/journals/mms/8-4/77109.html>

[†]Department of Mathematics, Florida International University, Miami, FL 33199 (khuang@fiu.edu).

[‡]Department of Mathematics, Purdue University, West Lafayette, IN 47907 (lpeijun@math.purdue.edu). The research of this author was supported in part by NSF grants EAR-0724656 and DMS-0914595.

is to be determined by adding to the incident beam the waves emitted by all other scatterers, and the waves emitted by those scatterers are in turn influenced by the radiation emitted by the scatterer in question. The specific procedure is not an expansion in different order of scattering. The field acting on a given scatterer or emitted by it includes the effects of all orders of scattering. This method effectively gives the wave fields by solving a linear system for the idealized situation, where the medium is viewed as a collection of isotropic point scatterers. Though there is a very complicated scattering picture with multiple scattering of all orders, the scattered field can be computed very efficiently.

Another basic problem in classical scattering theory is the scattering of time-harmonic acoustic or electromagnetic waves by a bounded impenetrable obstacle with scale comparable to the wavelength or larger. In view of differential equations, this problem can be reduced to an exterior boundary value problem. To apply numerical methods, the open domain needs to be truncated into a bounded domain. Therefore, a suitable boundary condition then has to be imposed on the boundary of the bounded domain so that no artificial wave reflection occurs. There are a variety of ways to provide such a “nonreflecting” boundary condition, e.g., nonlocal Dirichlet-to-Neumann maps, local absorbing boundary conditions as approximations to nonlocal Dirichlet-to-Neumann maps, perfectly matched layer techniques, and boundary integral equations. Integral equation methods play a central role in the study of boundary value problems associated with the scattering of acoustic or electromagnetic waves by bounded obstacles. This is primarily due to the fact that the mathematical formulation of such problems leads to equations defined over unbounded domains, and hence their reformulation in terms of boundary integral equations not only reduces the dimensionality of the problem but also allows one to replace a problem over an unbounded domain by one over a bounded domain. One may consult the book by Colton and Kress [5] for comprehensive accounts of the obstacle scattering problem.

More interestingly, in many situations one wishes to simulate wave propagation in a heterogeneous medium with different scales, e.g., extended obstacles embedded in randomly distributed small scale scatterers. This is the case when one wants to use the numerical schemes for assessment of methods for imaging in a cluttered environment. Therefore, we need to solve the direct scattering problem corresponding to wave propagation in the heterogeneous medium. This is a challenging problem which, in general, involves phenomena on many scales, in particular the scales of the medium variations, the wavelength, and the propagation distance. In this work, the clutter medium is modeled by a set of isotropic point scatterers and an extended obstacle with one or possibly more components, as seen in Figure 1. When the point scatterers and the extended obstacle are simultaneously illuminated by an incident wave, the scattered waves will be generated from the point scatterers and the extended obstacle, respectively. The scattered wave from the point scatterers will interact with the extended obstacle to induce further scattered fields; on the other hand, the scattered wave from the extended obstacle will also interact with the point scatterers to induce further scattered fields. Therefore, the field scattered from one side will induce further scattered fields from the other side, which will induce further scattered fields from the other side, and so on. This recursive way of thinking about how to calculate the total field leads to a notion of multiple scattering; it can be used to actually compute the total scattered field, and each step is called an order of scattering. Throughout the paper we consider a scalar wave field in the frequency domain so that the governing equation is the Helmholtz equation.

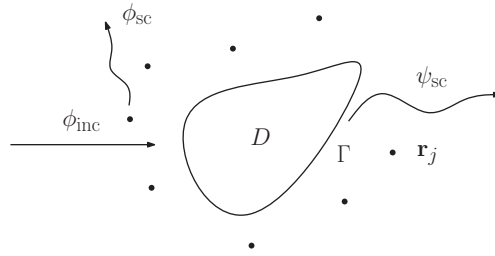


FIG. 1. Schematic of problem geometry. A plane wave is incident on the heterogeneous medium consisting of point scatterers centered at \mathbf{r}_j and an extended obstacle D with boundary Γ .

To compute the scattered field from the interaction between the incident wave and point scatterers only, the Foldy–Lax method provides an effective approach, while boundary integral equation methods play an important role for solving the scattering problem solely involving an extended obstacle. It is a challenging two-scale multiple scattering problem when both the point scatterers and the extended obstacle are present. The idea of the work is to combine these two methods such that the multiple scattering between the extended obstacle and the point scatterers can be fully taken into account, ideally without increasing significantly the computational complexity relative to the original algorithms. We develop a generalized Foldy–Lax method, which is viewed from two different formulations: the series solution and the integral equation. The series solution formulation is shown as an efficient iterative scheme to the integral equation formulation. The convergence of the scattered fields and the far-field patterns from the series solution formulation are characterized in terms of scattering coefficients. Numerical experiments are presented for two types of heterogeneous medium in three dimensions, uniformly distributed point scatterers surrounding the unit sphere, and randomly distributed point scatterers surrounding an obstacle with a rough surface. Recently, based on the null field or extended boundary condition approach and scattering operators, a generalized Foldy–Lax formulation was developed to solve the two-dimensional multiple scattering problem in [8], where the formulation is represented as a series in terms of spherical harmonics. The generalized Foldy–Lax formulation in the current paper is different from that in [8] since our approach is based on the boundary integral equation for a three-dimensional problem and therefore can be used to deal with obstacles with more general geometries.

The outline of the paper is as follows. In section 2, the Foldy–Lax method is briefly reviewed for computing the scattered wave fields arising from the interaction of the incident wave with the point scatterers; a model problem for the obstacle scattering problem is introduced, and a boundary integral equation is presented; and a generalized Foldy–Lax method with two formulations is developed to solve the two-scale multiple scattering problem when both the point scatterers and the extended obstacle are present. The convergence results of the scattered field and the far-field patterns for the series solution formulation are established in section 3. Numerical experiments are shown in section 4. The paper is concluded in section 5 with comments and directions for future work.

2. Multiple scattering system. In this section, we present a generalized Foldy–Lax formulation for the multiple scattering problem, which involves both the point scatterers and an extended obstacle. In this method, the multiple scattering between

the point scatterers and the extended obstacle is fully taken into account by combining the boundary integral equation method with the Foldy–Lax method.

2.1. Scattering from point scatterers. We briefly review the Foldy–Lax method for the scattering problem involving only the isotropic point scatterers. The waves scattered by any one scatterer will be represented by a point source located at some point within the scatterer.

Consider a collection of m separated point scatterers at $\mathbf{r}_1, \dots, \mathbf{r}_m$. Let ϕ_{inc} be the plane incident wave, given explicitly as

$$\phi_{\text{inc}}(\mathbf{r}) = e^{i\kappa\mathbf{r}\cdot\mathbf{d}} \quad \text{in } \mathbb{R}^3,$$

where i is the imaginary unit, κ is the wavenumber, and \mathbf{d} is the propagation direction defined on the unit sphere. Since the point scatterers are treated as isotropic, the scattered field in the neighborhood of the j th scatterer will behave like

$$A_j G(\mathbf{r}, \mathbf{r}_j),$$

where A_j is an unknown amplitude and G is the free-space Green's function satisfying

$$\Delta G(\mathbf{r}, \mathbf{r}') + \kappa^2 G(\mathbf{r}, \mathbf{r}') = -\delta(\mathbf{r} - \mathbf{r}') \quad \text{in } \mathbb{R}^3,$$

which is given explicitly in three dimensions as

$$G(\mathbf{r}, \mathbf{r}') = \frac{1}{4\pi} \frac{e^{i\kappa|\mathbf{r}-\mathbf{r}'|}}{|\mathbf{r}-\mathbf{r}'|}.$$

The total field is represented as the sum of the incident field and the scattered field,

$$(2.1) \quad \phi(\mathbf{r}) = \phi_{\text{inc}}(\mathbf{r}) + \sum_{j=1}^m A_j G(\mathbf{r}, \mathbf{r}_j).$$

The external field acting on the i th scatterer is defined as

$$(2.2) \quad \phi_{\text{ext},i}(\mathbf{r}) = \phi(\mathbf{r}) - A_i G(\mathbf{r}, \mathbf{r}_i) = \phi_{\text{inc}}(\mathbf{r}) + \sum_{\substack{j=1 \\ j \neq i}}^m A_j G(\mathbf{r}, \mathbf{r}_j).$$

It can be regarded as the field incident on the i th scatterer in the presence of all the other scatterers.

The scattering properties of the scatterers can be characterized by

$$(2.3) \quad A_i = \sigma_i \phi_{\text{ext},i}(\mathbf{r}_i),$$

which makes the strength of the scattered wave from a scatterer proportional to the external field acting on it. Here σ_i is referred to as the scattering coefficient for the

i th scatterer. The scattering coefficients characterize how the point scatterer excites waves and can be determined from enforcing energy conservation. Thus, the scattered field is determined by the value of the external field at the center of the scatterer \mathbf{r}_i together with the quantity σ_i .

Using (2.3) and evaluating (2.2) at \mathbf{r}_i yields

$$(2.4) \quad \phi_{\text{ext},i}(\mathbf{r}_i) = \phi_{\text{inc}}(\mathbf{r}_i) + \sum_{\substack{j=1 \\ j \neq i}}^m \sigma_j \phi_{\text{ext},j}(\mathbf{r}_j) G(\mathbf{r}_i, \mathbf{r}_j),$$

which is a linear system of algebraic equations for $\phi_{\text{ext},j}(\mathbf{r}_j)$ and represents the fundamental equations of multiple scattering for a set of point scatterers.

Equivalently we have from (2.4) that

$$\sigma_i^{-1} A_i = \phi_{\text{inc}}(\mathbf{r}_i) + \sum_{\substack{j=1 \\ j \neq i}}^m A_j G(\mathbf{r}_i, \mathbf{r}_j),$$

which can be written in the form

$$(2.5) \quad MA = \phi_{\text{sou}}.$$

Here $A = [A_1, A_2, \dots, A_m]^\top$ is the amplitude vector, $\phi_{\text{sou}} = [\phi_{\text{inc}}(\mathbf{r}_1), \phi_{\text{inc}}(\mathbf{r}_2), \dots, \phi_{\text{inc}}(\mathbf{r}_m)]^\top$ is the source field vector, and the $m \times m$ coefficient matrix M is

$$M = \begin{bmatrix} \sigma_1^{-1} & -G(\mathbf{r}_1, \mathbf{r}_2) & \cdots & -G(\mathbf{r}_1, \mathbf{r}_m) \\ -G(\mathbf{r}_2, \mathbf{r}_1) & \sigma_2^{-1} & \cdots & -G(\mathbf{r}_2, \mathbf{r}_m) \\ \vdots & \vdots & \ddots & \vdots \\ -G(\mathbf{r}_m, \mathbf{r}_1) & -G(\mathbf{r}_m, \mathbf{r}_2) & \cdots & \sigma_m^{-1} \end{bmatrix}.$$

After solving the above linear system for A , the total field can be obtained from (2.1), and the scattered field can be expressed as

$$(2.6) \quad \phi_{\text{sc}}(\mathbf{r}) = \sum_{j=1}^m A_j G(\mathbf{r}, \mathbf{r}_j).$$

Remark 2.1. For a single point scatterer at \mathbf{r}_0 , the linear system (2.5) is reduced to the identity

$$A_0 = \sigma_0 \phi_{\text{inc}}(\mathbf{r}_0).$$

The scattered field is simply given by

$$\phi_{\text{sc}}(\mathbf{r}) = \sigma_0 \phi_{\text{inc}}(\mathbf{r}_0) G(\mathbf{r}, \mathbf{r}_0),$$

where σ_0 is the scattering coefficient for the single point scatterer.

Next we examine the invertibility of the coefficient matrix M and estimate the bound of its inverse. We begin with a useful lemma.

LEMMA 2.1. *If B and $B - D$ are nonsingular matrices, then*

$$(B - D)^{-1} = B^{-1} + B^{-1}(I - DB^{-1})^{-1}DB^{-1}.$$

Proof. The proof is done by verifying

$$[B - D][B^{-1} + B^{-1}(I - DB^{-1})^{-1}DB^{-1}] = I. \quad \square$$

Given a vector $\mathbf{x} = (x_1, x_2, \dots, x_m)^\top \in \mathbb{C}^m$ and a matrix $B = [b_{ij}]_{m \times m} \in \mathbb{C}^{m \times m}$, introduce the maximum norms

$$\|\mathbf{x}\|_\infty := \max_{1 \leq j \leq m} |x_j| \quad \text{and} \quad \|B\|_\infty := \max_{1 \leq i \leq m} \sum_{j=1}^m |b_{ij}|.$$

Define an important parameter

$$\sigma_{\max} := \max_{1 \leq j \leq m} |\sigma_j|.$$

This parameter describes the strength of the scattered waves from the point scatterers and will be used to characterize the convergence of the generalized Foldy–Lax method.

THEOREM 2.1. *If σ_{\max} is small enough, the coefficient matrix M is invertible and has the estimate*

$$(2.7) \quad \|M^{-1}\|_\infty \leq C\sigma_{\max},$$

where C is independent of σ_j for $j = 1, 2, \dots, m$.

Proof. Split the matrix $M = M_1 - M_2$, where

$$M_1 = \begin{bmatrix} \sigma_1^{-1} & & & \\ & \sigma_2^{-1} & & \\ & & \ddots & \\ & & & \sigma_m^{-1} \end{bmatrix} \quad \text{and}$$

$$M_2 = \begin{bmatrix} 0 & G(\mathbf{r}_1, \mathbf{r}_2) & \cdots & G(\mathbf{r}_1, \mathbf{r}_m) \\ G(\mathbf{r}_2, \mathbf{r}_1) & 0 & \cdots & G(\mathbf{r}_2, \mathbf{r}_m) \\ \vdots & \vdots & \ddots & \vdots \\ G(\mathbf{r}_m, \mathbf{r}_1) & G(\mathbf{r}_m, \mathbf{r}_2) & \cdots & 0 \end{bmatrix}.$$

Evidently, the matrix M_1 is invertible. We have from the properties of the matrix norm that

$$\|M_2M_1^{-1}\|_\infty \leq \|M_2\|_\infty \|M_1^{-1}\|_\infty = \sigma_{\max} \|M_2\|_\infty < 1$$

as σ_{\max} is small enough. The above estimate indicates that the matrix $I - M_2M_1^{-1}$ or equivalently the matrix $M = M_1 - M_2$ is invertible, and furthermore we have the estimate

$$\|I - M_2M_1^{-1}\|_\infty \leq \frac{1}{1 - \|M_2M_1^{-1}\|_\infty} \leq \frac{1}{1 - \sigma_{\max} \|M_2\|_\infty}.$$

It follows from Lemma 2.1 that

$$M^{-1} = (M_1 - M_2)^{-1} = M_1^{-1} + M_1^{-1}(I - M_2M_1^{-1})^{-1}M_2M_1^{-1}.$$

Following the same argument for small enough σ_{\max} gives

$$\begin{aligned} \| M^{-1} \|_{\infty} &= \| M_1^{-1} + M_1^{-1}(I - M_2M_1^{-1})^{-1}M_2M_1^{-1} \|_{\infty} \\ &\leq \| M_1^{-1} \|_{\infty} + \| M_1^{-1} \|_{\infty} \frac{\| M_2M_1^{-1} \|_{\infty}}{1 - \| M_2M_1^{-1} \|_{\infty}} \\ &\leq \| M_1^{-1} \|_{\infty} \left(1 + \frac{\| M_2M_1^{-1} \|_{\infty}}{1 - \| M_2M_1^{-1} \|_{\infty}} \right) \\ &\leq \sigma_{\max} \left(1 + \frac{\sigma_{\max} \| M_2 \|_{\infty}}{1 - \sigma_{\max} \| M_2 \|_{\infty}} \right) \leq C\sigma_{\max}. \quad \square \end{aligned}$$

Given m separated point scatterers at \mathbf{r}_j , if σ_{\max} is small, we may have from (2.4) that

$$\phi_{\text{ext},i}(\mathbf{r}_i) \approx \phi_{\text{inc}}(\mathbf{r}_i),$$

which gives an approximation to the scattered field

$$\phi_{\text{sc}}(\mathbf{r}) \approx \sum_{j=1}^m \sigma_j \phi_{\text{inc}}(\mathbf{r}_j) G(\mathbf{r}, \mathbf{r}_j).$$

In this case, the interaction among the m point scatterers is weak. Therefore the parameter σ_{\max} characterizes the situation when the weak scattering occurs.

2.2. Scattering from an extended obstacle. This section is devoted to the solution of the obstacle scattering problem. More specifically, we consider the scattering of time-harmonic acoustic waves by a bounded sound-soft impenetrable obstacle. In this section, if not stated otherwise, we always will assume that the obstacle is represented by the domain D with boundary Γ , which is the open complement of an unbounded domain of class C^2 , i.e., scattering from more than one component is included in our analysis.

Consider the Helmholtz equation,

$$(2.8) \quad \Delta\psi + \kappa^2\psi = 0 \quad \text{in } \mathbb{R}^3 \setminus \overline{D},$$

along with the sound-soft boundary condition

$$(2.9) \quad \psi = 0 \quad \text{on } \Gamma,$$

where ψ is the total field and κ is a positive real number and is called the wavenumber as before. Boundary conditions other than sound-soft, e.g., sound-hard or impedance boundary condition, can be considered similarly.

The obstacle is illuminated by the same plane incident wave as that incident on the point scatterers. The total field ψ consists of the incident field ϕ_{inc} and the scattered ψ_{sc} :

$$(2.10) \quad \psi = \phi_{\text{inc}} + \psi_{\text{sc}}.$$

It follows from (2.8)–(2.10) that the scattered field satisfies

$$\Delta\psi_{\text{sc}} + \kappa^2\psi_{\text{sc}} = 0 \quad \text{in } \mathbb{R}^3 \setminus \overline{D},$$

together with the boundary condition

$$\psi_{\text{sc}} = -\phi_{\text{inc}} \quad \text{on } \Gamma.$$

In addition, the scattered field is required to satisfy the Sommerfeld radiation condition

$$\lim_{\rho \rightarrow \infty} \sqrt{\rho} \left(\frac{\partial \psi_{\text{sc}}}{\partial \rho} - i\kappa \psi_{\text{sc}} \right) = 0, \quad \rho = |\mathbf{r}|,$$

uniformly for all directions $\hat{\mathbf{r}} = \mathbf{r}/|\mathbf{r}|$.

Next we present a boundary integral equation method to solve the above exterior boundary value problem. The main advantage of the use of boundary integral equation methods to study exterior boundary value problems lies in the fact that this approach reduces a problem defined over an unbounded domain to one defined on a bounded domain of lower dimension, i.e., the boundary of the scattering obstacle.

It follows immediately from Green's representation theorem that

$$\psi_{\text{sc}}(\mathbf{r}) = \int_{\Gamma} \partial_{\mathbf{n}'} G(\mathbf{r}, \mathbf{r}') \psi_{\text{sc}}(\mathbf{r}') ds(\mathbf{r}') - \int_{\Gamma} G(\mathbf{r}, \mathbf{r}') \partial_{\mathbf{n}'} \psi_{\text{sc}}(\mathbf{r}') ds(\mathbf{r}'), \quad \mathbf{r} \in \mathbb{R}^3 \setminus \overline{D},$$

where \mathbf{n}' is the unit outward normal with respect to the variable \mathbf{r}' and is assumed to be directed into the exterior of D .

Similarly we have for the incident field that

$$0 = \int_{\Gamma} \partial_{\mathbf{n}'} G(\mathbf{r}, \mathbf{r}') \phi_{\text{inc}}(\mathbf{r}') ds(\mathbf{r}') - \int_{\Gamma} G(\mathbf{r}, \mathbf{r}') \partial_{\mathbf{n}'} \phi_{\text{inc}}(\mathbf{r}') ds(\mathbf{r}'), \quad \mathbf{r} \in \mathbb{R}^3 \setminus \overline{D}.$$

Adding these two equations and using the boundary condition (2.9) gives

$$(2.11) \quad \psi_{\text{sc}}(\mathbf{r}) = - \int_{\Gamma} G(\mathbf{r}, \mathbf{r}') \partial_{\mathbf{n}'} \psi(\mathbf{r}') ds(\mathbf{r}'), \quad \mathbf{r} \in \mathbb{R}^3 \setminus \overline{D}.$$

To compute the scattered field, the normal derivative of the total field, $\partial_{\mathbf{n}}\psi$, needs to be determined on the boundary Γ . Adding the incident field on both sides of (2.11), using the potential theory, and taking the normal derivative on the boundary Γ , we obtain the boundary integral equation

$$(2.12) \quad \frac{1}{2} \partial_{\mathbf{n}} \psi(\mathbf{r}) + \int_{\Gamma} \partial_{\mathbf{n}} G(\mathbf{r}, \mathbf{r}') \partial_{\mathbf{n}'} \psi(\mathbf{r}') ds(\mathbf{r}') = \partial_{\mathbf{n}} \phi_{\text{inc}}(\mathbf{r}).$$

It is known that (2.12) is not uniquely solvable at the eigenvalues of the corresponding interior boundary value problem. Several attempts have been made to

alleviate the problem of spurious resonances, including the combined field equations. For example, the following uniquely solvable boundary integral equation by Brakhage and Werner [2] may be considered,

$$\frac{1}{2} \partial_{\mathbf{n}} \psi(\mathbf{r}) + \int_{\Gamma} [\partial_{\mathbf{n}} G(\mathbf{r}, \mathbf{r}') + i\eta G(\mathbf{r}, \mathbf{r}')] \partial_{\mathbf{n}'} \psi(\mathbf{r}') ds(\mathbf{r}') = (\partial_{\mathbf{n}} + i\eta) \phi_{\text{inc}}(\mathbf{r}),$$

where \mathbf{n} is the unit outward normal with respect to the variable \mathbf{r} . Here η is a nonzero real number and is called the coupling parameter. For an investigation on the proper choice of the coupling parameter η with respect to the condition number of the coefficient matrix for the integral equation, we refer to Kress [9]. However, we feel that the alternative approach makes the arguments a little more complicated since our main intention is to derive a generalized Foldy–Lax formulation which accounts for the presence of the extended obstacle. Therefore, we will use boundary integral equation (2.12) and assume that it is uniquely solvable throughout the paper.

Given a domain Ω , define

$$\| u \|_{0,\infty,\Omega} := \sup_{\mathbf{r} \in \Omega} |u(\mathbf{r})|.$$

Introduce a standard Sobolev space

$$W^{1,\infty}(\Omega) := \{u \in L^1_{\text{loc}}(\Omega) : \| u \|_{1,\infty,\Omega} \leq \infty\},$$

where the Sobolev norm is

$$\| u \|_{1,\infty,\Omega} := \max_{|\alpha| \leq 1} \| D^\alpha u \|_{0,\infty,\Omega}.$$

In order to prove the stability of the solution for the boundary integral equation (2.12), we need the following classical result, which may be found in Colton and Kress [5].

LEMMA 2.2. *Let X be a normed space, $T : X \rightarrow X$ be a compact operator, and $I + T$ be injective. Then the inverse operator $(I + T)^{-1} : X \rightarrow X$ exists and is bounded.*

THEOREM 2.2. *The solution to the boundary integral equation (2.12) depends continuously on the incident field, i.e.,*

$$(2.13) \quad \| \partial_{\mathbf{n}} \psi \|_{0,\infty,\Gamma} \leq C \| \phi_{\text{inc}} \|_{1,\infty,\Gamma},$$

where C depends on η and Γ .

Proof. Introduce the double-layer potential operator $K : W^{0,\infty}(\Gamma) \rightarrow W^{0,\infty}(\Gamma)$ by

$$(Ku)(\mathbf{r}) := \int_{\Gamma} \partial_{\mathbf{n}} G(\mathbf{r}, \mathbf{r}') u(\mathbf{r}') ds(\mathbf{r}').$$

The integral equation (2.12) can be written as

$$(2.14) \quad \left(\frac{1}{2} I + K \right) \partial_{\mathbf{n}} \psi = \partial_{\mathbf{n}} \psi_{\text{inc}}.$$

It follows from the compactness of the operator K , along with Lemma 2.2, that

$$\| \partial_{\mathbf{n}} \psi \|_{0,\infty,\Gamma} \leq C \| \partial_{\mathbf{n}} \psi_{\text{inc}} \|_{0,\infty,\Gamma} \leq C \| \phi_{\text{inc}} \|_{1,\infty,\Gamma}. \quad \square$$

2.3. Series solution formulation. This section is concerned with a series solution formulation for the multiple scattering between the extended obstacle and the point scatterers. The field scattered from one obstacle will induce further scattered fields from all the other obstacles, which will induce further scattered fields from all the other obstacles, and so on. The multiple scattering can be regarded as the summation of all the orders of scattering. The series solution formulation provides us a physical instinct on how the multiple scattering occurs. In the following, we consider the scattering orders one by one.

The first order scattering is

$$u_{\text{sc}}^{(1)}(\mathbf{r}) = \phi_{\text{sc}}^{(1)}(\mathbf{r}) + \psi_{\text{sc}}^{(1)}(\mathbf{r}),$$

where $\phi_{\text{sc}}^{(1)}$ and $\psi_{\text{sc}}^{(1)}$ are the scattered fields from the interaction of the incident field with the point scatterers and the extended obstacle, respectively. They satisfy from (2.6) and (2.11)

$$(2.15) \quad \phi_{\text{sc}}^{(1)}(\mathbf{r}) = \sum_{j=1}^m A_j^{(1)} G(\mathbf{r}, \mathbf{r}_j),$$

$$(2.16) \quad \psi_{\text{sc}}^{(1)}(\mathbf{r}) = - \int_{\Gamma} G(\mathbf{r}, \mathbf{r}') \partial_{\mathbf{n}'} \psi^{(1)}(\mathbf{r}') ds(\mathbf{r}'),$$

where $A_j^{(1)}$ and $\partial_{\mathbf{n}} \psi^{(1)}$ are the solutions of the following equations:

$$\begin{aligned} MA^{(1)} &= \phi_{\text{sou}}^{(0)}, \\ \left(\frac{1}{2}I + K\right) \partial_{\mathbf{n}} \psi^{(1)} &= \psi_{\text{sou}}^{(0)}. \end{aligned}$$

Here the source fields of order 0 take the forms

$$\begin{aligned} \phi_{\text{sou}}^{(0)} &= [\phi_{\text{inc}}(\mathbf{r}_1), \dots, \phi_{\text{inc}}(\mathbf{r}_m)]^{\top}, \\ \psi_{\text{sou}}^{(0)} &= \partial_{\mathbf{n}} \phi_{\text{inc}}. \end{aligned}$$

The second order scattering is induced by the first order scattering and can be written as

$$u_{\text{sc}}^{(2)}(\mathbf{r}) = \phi_{\text{sc}}^{(2)}(\mathbf{r}) + \psi_{\text{sc}}^{(2)}(\mathbf{r}),$$

where $\phi_{\text{sc}}^{(2)}$ is the scattered field due to the interaction of the point scatterers with the first order scattered field from the extended obstacle, while $\psi_{\text{sc}}^{(2)}$ is the scattered field due to the interaction of the extended obstacle with the first order scattered field from the point scatterers. Specifically, it follows again from (2.6) and (2.11) that

$$\begin{aligned} \phi_{\text{sc}}^{(2)}(\mathbf{r}) &= \sum_{j=1}^m A_j^{(2)} G(\mathbf{r}, \mathbf{r}_j), \\ \psi_{\text{sc}}^{(2)}(\mathbf{r}) &= - \int_{\Gamma} G(\mathbf{r}, \mathbf{r}') \partial_{\mathbf{n}'} \psi^{(2)}(\mathbf{r}') ds(\mathbf{r}'). \end{aligned}$$

Here $A^{(2)}$ and $\partial_{\mathbf{n}} \psi^{(2)}$ are the solutions of the following equations:

$$\begin{aligned} MA^{(2)} &= \phi_{\text{sou}}^{(1)}, \\ \left(\frac{1}{2}I + K\right) \partial_{\mathbf{n}} \psi^{(2)} &= \psi_{\text{sou}}^{(1)}, \end{aligned}$$

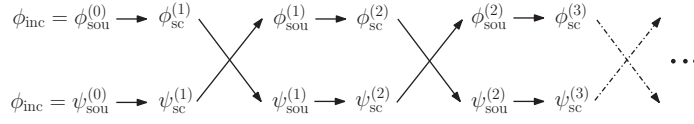


FIG. 2. Schematic of the process for the series solution formulation.

where the source fields of order 1 are given as

$$\phi_{\text{sou}}^{(1)} = [\psi_{\text{sc}}^{(1)}(\mathbf{r}_1), \dots, \psi_{\text{sc}}^{(1)}(\mathbf{r}_m)]^\top,$$

$$\psi_{\text{sou}}^{(1)} = \partial_{\mathbf{n}} \phi_{\text{sc}}^{(1)}.$$

Repeating the above process leads to the general expression of the k th order scattering

$$u_{\text{sc}}^{(k)}(\mathbf{r}) = \phi_{\text{sc}}^{(k)}(\mathbf{r}) + \psi_{\text{sc}}^{(k)}(\mathbf{r}),$$

where

$$(2.17) \quad \phi_{\text{sc}}^{(k)}(\mathbf{r}) = \sum_{j=1}^m A_j^{(k)} G(\mathbf{r}, \mathbf{r}_j),$$

$$(2.18) \quad \psi_{\text{sc}}^{(k)}(\mathbf{r}) = - \int_{\Gamma} G(\mathbf{r}, \mathbf{r}') \partial_{\mathbf{n}'} \psi^{(k)}(\mathbf{r}') ds(\mathbf{r}').$$

Here $A^{(k)}$ and $\partial_{\mathbf{n}} \psi^{(k)}$ are the solutions of the following equations:

$$(2.19) \quad MA^{(k)} = \phi_{\text{sou}}^{(k-1)},$$

$$(2.20) \quad \left(\frac{1}{2}I + K\right) \partial_{\mathbf{n}} \psi^{(k)} = \psi_{\text{sou}}^{(k-1)},$$

where the source fields of order $k - 1$ are expressed as

$$(2.21) \quad \phi_{\text{sou}}^{(k-1)} = [\psi_{\text{sc}}^{(k-1)}(\mathbf{r}_1), \dots, \psi_{\text{sc}}^{(k-1)}(\mathbf{r}_m)]^\top,$$

$$(2.22) \quad \psi_{\text{sou}}^{(k-1)} = \partial_{\mathbf{n}} \phi_{\text{sc}}^{(k-1)}.$$

The above process can be described as in Figure 2: the incident field ϕ_{inc} , as an initial source $\phi_{\text{sou}}^{(0)}$, interacts with the point scatterers and generates the first order scattered field $\phi_{\text{sc}}^{(1)}$. The first order scattered field due to the point scatterers $\phi_{\text{sc}}^{(1)}$, as a source $\psi_{\text{sou}}^{(1)}$, interacts with the extended obstacle and generates the scattered field $\psi_{\text{sc}}^{(2)}$, which is treated as a source $\phi_{\text{sou}}^{(2)}$ and interacts with the point scatterers to generate the scattered field $\phi_{\text{sc}}^{(3)}$, and so on; on the other hand, the incident field ϕ_{inc} , as an initial source $\psi_{\text{sou}}^{(0)}$, interacts with the extended obstacle and generates the first order scattered field $\psi_{\text{sc}}^{(1)}$. The first order scattered field due to the extended obstacle $\psi_{\text{sc}}^{(1)}$, as a source $\phi_{\text{sou}}^{(1)}$, interacts with the point scatterers and generates the scattered field $\phi_{\text{sc}}^{(2)}$, which is treated as a source $\psi_{\text{sou}}^{(2)}$ and interacts with the extended obstacle to generate the scattered field $\psi_{\text{sc}}^{(3)}$, and so on.

Denote u_{sc}^p and u_{sc}^o as the portions of the scattered fields contributed from the point scatterers and the extended obstacle, respectively. They may be defined as the

limit of the following partial sums:

$$\begin{aligned} u_{\text{sc}}^{\text{p}} &= \lim_{k \rightarrow \infty} \left[\phi_{\text{sc}}^{(1)} + \phi_{\text{sc}}^{(2)} + \cdots + \phi_{\text{sc}}^{(k)} \right], \\ u_{\text{sc}}^{\text{o}} &= \lim_{k \rightarrow \infty} \left[\psi_{\text{sc}}^{(1)} + \psi_{\text{sc}}^{(2)} + \cdots + \psi_{\text{sc}}^{(k)} \right]. \end{aligned}$$

The total scattered field can thus be represented as the summation of the two portions

$$\begin{aligned} u_{\text{sc}} &= \lim_{k \rightarrow \infty} \left[u_{\text{sc}}^{(1)} + u_{\text{sc}}^{(2)} + \cdots + u_{\text{sc}}^{(k)} \right] \\ &= \lim_{k \rightarrow \infty} \left[\phi_{\text{sc}}^{(1)} + \phi_{\text{sc}}^{(2)} + \cdots + \phi_{\text{sc}}^{(k)} \right] + \lim_{k \rightarrow \infty} \left[\psi_{\text{sc}}^{(1)} + \psi_{\text{sc}}^{(2)} + \cdots + \psi_{\text{sc}}^{(k)} \right] \\ &= u_{\text{sc}}^{\text{p}} + u_{\text{sc}}^{\text{o}}. \end{aligned}$$

2.4. Integral equation formulation. This section is concerned with the generalized Foldy–Lax method from another point of view and presents a compact integral equation formulation. Furthermore, it is shown that the series solution formulation actually describes an iterative scheme for solving the derived integral equation. Here we consider the same obstacle as that in previous sections, i.e., an impenetrable object with vanishing Dirichlet boundary condition.

Viewing the excited field due to the point scatterers as an external source field for the obstacle, we consider the Helmholtz equation for the total field

$$\Delta u + \kappa^2 u = - \sum_{j=1}^m \sigma_j u_j \delta(\mathbf{r} - \mathbf{r}_j) \quad \text{in } \mathbb{R}^3 \setminus \overline{D},$$

along with the sound-soft boundary condition

$$u = 0 \quad \text{on } \Gamma.$$

Subtracting the incident field from the total field, we may obtain the equation for the scattered field

$$\Delta u_{\text{sc}} + \kappa^2 u_{\text{sc}} = - \sum_{j=1}^m \sigma_j u_j \delta(\mathbf{r} - \mathbf{r}_j) \quad \text{in } \mathbb{R}^3 \setminus \overline{D}.$$

The scattered field is also required to satisfy the Sommerfeld radiation condition.

We derive an integral equation for solving the above exterior boundary value problem involving both the point scatterers and the extended obstacle.

It follows from Green's theorem that the scattered field has the following representation:

$$(2.23) \quad u_{\text{sc}}(\mathbf{r}) = \sum_{j=1}^m \sigma_j u_j G(\mathbf{r}, \mathbf{r}_j) - \int_{\Gamma} G(\mathbf{r}, \mathbf{r}') \partial_{\mathbf{n}'} u(\mathbf{r}') ds(\mathbf{r}'), \quad \mathbf{r} \in \mathbb{R}^3 \setminus \overline{D}.$$

Adding the incident field on both sides yields

$$(2.24) \quad u(\mathbf{r}) = \phi_{\text{inc}}(\mathbf{r}) + \sum_{j=1}^m \sigma_j u_j G(\mathbf{r}, \mathbf{r}_j) - \int_{\Gamma} G(\mathbf{r}, \mathbf{r}') \partial_{\mathbf{n}'} u(\mathbf{r}') ds(\mathbf{r}'), \quad \mathbf{r} \in \mathbb{R}^3 \setminus \overline{D}.$$

To compute the total field u at any point $\mathbf{r} \in \mathbb{R}^3 \setminus \overline{D}$, it is required to determine the excited field vector $[u_1, \dots, u_m]^\top$ and the normal derivative of the total field $\partial_{\mathbf{n}}u$ on the boundary of the obstacle Γ .

Evaluating (2.24) on both sides at \mathbf{r}_i gives

$$(2.25) \quad u_i = \phi_{\text{inc}}(\mathbf{r}_i) + \sum_{\substack{j=1 \\ j \neq i}}^m \sigma_j u_j G(\mathbf{r}_i, \mathbf{r}_j) - \int_{\Gamma} G(\mathbf{r}_i, \mathbf{r}') \partial_{\mathbf{n}'} u(\mathbf{r}') ds(\mathbf{r}').$$

Using the jump relation for the single-layer potential and taking the normal derivative, we obtain a boundary integral equation on Γ :

$$(2.26) \quad \frac{1}{2} \partial_{\mathbf{n}} u(\mathbf{r}) = \partial_{\mathbf{n}} u_{\text{inc}}(\mathbf{r}) + \sum_{j=1}^m \sigma_j u_j \partial_{\mathbf{n}} G(\mathbf{r}, \mathbf{r}_j) - \int_{\Gamma} \partial_{\mathbf{n}} G(\mathbf{r}, \mathbf{r}') \partial_{\mathbf{n}'} u(\mathbf{r}') ds(\mathbf{r}').$$

Equations (2.25) and (2.26) are the new self-consistent Foldy–Lax formulation in the case where both the point scatterers and the extended obstacle are present.

Remark 2.2. If the extended obstacle is not present, the boundary integral over Γ vanishes in (2.25), which reduces to the Foldy–Lax formulation (2.4); on the other hand, if the point scatterers are not present, the summation over the number of point scatterers vanishes in (2.26), which reduces to the regular boundary integral equation (2.12) for solving the obstacle scattering problem.

Next we show that the series solution formulation derived in the previous section actually describes an iterative method to solve the new self-consistent Foldy–Lax formulation (2.25) and (2.26). The nature of the method is similar to the Jacobi iterative method for solving a linear system.

First we describe the initial step. Consider (2.25) without the integral term and (2.26) without the summation term, respectively:

$$u_i^{(1)} - \sum_{\substack{j=1 \\ j \neq i}}^m \sigma_j u_j^{(1)} G(\mathbf{r}_i, \mathbf{r}_j) = \phi_{\text{inc}}(\mathbf{r}_i),$$

$$\frac{1}{2} \partial_{\mathbf{n}} u^{(1)}(\mathbf{r}) + \int_{\Gamma} \partial_{\mathbf{n}} G(\mathbf{r}, \mathbf{r}') \partial_{\mathbf{n}'} u^{(1)}(\mathbf{r}') ds(\mathbf{r}') = \partial_{\mathbf{n}} \phi_{\text{inc}}(\mathbf{r}).$$

After solving the above two equations, we obtain $[u_1^{(1)}, \dots, u_m^{(1)}]^\top$ and $\partial_{\mathbf{n}} u^{(1)}$ on Γ . They generate the first order scattered fields due to the point scatterers and the extended obstacle, which are exactly the same first order scattered fields as those from the series solution formulation in (2.15) and (2.16):

$$\phi_{\text{sc}}^{(1)} = \sum_{j=1}^m \sigma_j u_j^{(1)} G(\mathbf{r}, \mathbf{r}_j) \quad \text{and} \quad \psi_{\text{sc}}^{(1)} = - \int_{\Gamma} G(\mathbf{r}, \mathbf{r}') \partial_{\mathbf{n}'} u^{(1)}(\mathbf{r}') ds(\mathbf{r}').$$

To get correction terms, i.e., higher order scattering terms, we may use the iterative scheme

$$u_i^{(k)} - \sum_{\substack{j=1 \\ j \neq i}}^m \sigma_j u_j^{(k)} G(\mathbf{r}_i, \mathbf{r}_j) = - \int_{\Gamma} G(\mathbf{r}, \mathbf{r}') \partial_{\mathbf{n}'} u^{(k-1)}(\mathbf{r}') ds(\mathbf{r}'),$$

$$\frac{1}{2} \partial_{\mathbf{n}} u^{(k)}(\mathbf{r}) + \int_{\Gamma} \partial_{\mathbf{n}} G(\mathbf{r}, \mathbf{r}') \partial_{\mathbf{n}'} u^{(k)}(\mathbf{r}') ds(\mathbf{r}') = \sum_{j=1}^m \sigma_j u_j^{(k-1)} \partial_{\mathbf{n}} G(\mathbf{r}, \mathbf{r}_j)$$

for $k = 2, 3, \dots$. At k th step, we obtain the k th order scattered fields due to the point scatterers and the extended obstacle:

$$\phi_{sc}^{(k)} = \sum_{j=1}^m \sigma_j u_j^{(k)} G(\mathbf{r}, \mathbf{r}_j) \quad \text{and} \quad \psi_{sc}^{(k)} = - \int_{\Gamma} G(\mathbf{r}, \mathbf{r}') \partial_{\mathbf{n}'} u^{(k)}(\mathbf{r}') ds(\mathbf{r}').$$

Compared with (2.17) and (2.18), they are the k th terms in the series solution formulation. Therefore we have shown term by term that the series solution formulation indeed describes an iterative scheme to solve the self-consistent system (2.25) and (2.26), which is called the generalized Foldy–Lax formulation for dealing with the scattering problem involving both the point scatterers and an extended obstacle.

3. Convergence analysis. In this section, we analyze the convergence of the scattered fields and the far-field patterns from the series solution formulation for the multiple scattering problem.

3.1. Scattered fields. In the multiple scattering problem, the total scattered field is composed of the scattered field u_{sc}^p contributed from the point scatterers and the scattered field u_{sc}^e contributed from the extended obstacle. We will consider the convergence of the infinite series derived in the previous section for the scattered fields u_{sc}^p and u_{sc}^e separately. The idea is to deduce that the infinite series is dominated by a geometrical series.

Based on the general expression of the k th order scattering from (2.17)–(2.22), we conclude that it suffices to estimate the k th order scattered fields $\phi_{sc}^{(k)}$ on the boundary of the obstacle Γ and $\psi_{sc}^{(k)}$ at the position of the point scatterers $\mathbf{r}_j, j = 1, \dots, m$.

First consider $\phi_{sc}^{(k)}$. It follows from (2.17) that

$$(3.1) \quad \|\phi_{sc}^{(k)}\|_{1,\infty,\Gamma} = \left\| \sum_{j=1}^m A_j^{(k)} G(\mathbf{r}, \mathbf{r}_j) \right\|_{1,\infty,\Gamma} \leq C_1 \|A^{(k)}\|_{\infty},$$

where $\|\cdot\|_{\infty}$ is the vector maximum norm and

$$C_1 = \sum_{j=1}^m \|G(\cdot, \mathbf{r}_j)\|_{1,\infty,\Gamma},$$

which is a fixed constant once the positions of the point scatterers are fixed.

Applying Theorem 2.1 to (2.19) yields

$$(3.2) \quad \|A^{(k)}\|_{\infty} \leq C_2 \sigma_{\max} \|\phi_{\text{sou}}^{(k-1)}\|_{\infty},$$

where the constant C_2 plays the role of the constant C in (2.7).

The vector maximum norm gives

$$(3.3) \quad \|\phi_{\text{sou}}^{(k-1)}\|_{\infty} = \max_{1 \leq j \leq m} |\psi_{sc}^{(k-1)}(\mathbf{r}_j)| = \|\psi_{sc}^{(k-1)}\|_{\infty}.$$

Replacing the index k by $k - 1$ in (2.18) and evaluating at \mathbf{r}_j on both sides lead to

$$(3.4) \quad \|\psi_{sc}^{(k-1)}\|_{\infty} \leq C_3 \|\partial_{\mathbf{n}} \psi^{(k-1)}\|_{0,\infty,\Gamma},$$

where

$$C_3 = \max_{1 \leq j \leq m} \int_{\Gamma} |G(\mathbf{r}, \mathbf{r}_j)| ds(\mathbf{r}),$$

which is also a fixed constant once the point scatterers and the extended obstacle are given.

We have from Theorem 2.2 that

$$(3.5) \quad \|\partial_{\mathbf{n}}\psi^{(k-1)}\|_{0,\infty,\Gamma} \leq C_4 \|\phi_{\text{sc}}^{(k-2)}\|_{1,\infty,\Gamma},$$

where the constant C_4 plays the role of the constant C in (2.15).

Combining (3.1)–(3.5) yields

$$(3.6) \quad \|\phi_{\text{sc}}^{(k)}\|_{1,\infty,\Gamma} \leq C\sigma_{\text{max}} \|\phi_{\text{sc}}^{(k-2)}\|_{1,\infty,\Gamma},$$

where the constant

$$C = \prod_{i=1}^4 C_i$$

is independent of σ_{max} . When σ_{max} is small enough so that $C\sigma_{\text{max}}$ is less than unity, it is expected that the infinite series $\phi_{\text{sc}}^{(k)}$ is dominated by a geometrical series, and thus the convergence is followed.

Next consider $\psi_{\text{sc}}^{(k)}$. We have from (2.18) that

$$(3.7) \quad \|\psi_{\text{sc}}^{(k)}\|_{\infty} = \max_{1 \leq j \leq m} |\psi_{\text{sc}}^{(k)}(\mathbf{r}_j)| \leq C_3 \|\partial_{\mathbf{n}}\psi^{(k)}\|_{0,\infty,\Gamma}.$$

Theorem 2.2 implies again

$$(3.8) \quad \|\partial_{\mathbf{n}}\psi^{(k)}\|_{0,\infty,\Gamma} \leq C_4 \|\phi_{\text{sc}}^{(k-1)}\|_{1,\infty,\Gamma}.$$

Replacing the index k by $k - 1$ in (2.17) yields

$$(3.9) \quad \|\phi_{\text{sc}}^{(k-1)}\|_{1,\infty,\Gamma} = \left\| \sum_{j=1}^m A_j^{(k-1)} G(\mathbf{r}, \mathbf{r}_j) \right\|_{1,\infty,\Gamma} \leq C_1 \|A^{(k-1)}\|_{\infty}.$$

An application of Theorem 2.1 gives

$$(3.10) \quad \|A^{(k-1)}\|_{\infty} \leq C_2\sigma_{\text{max}} \|\phi_{\text{sou}}^{(k-2)}\|_{\infty}.$$

It follows from (2.21) that

$$(3.11) \quad \|\phi_{\text{sou}}^{(k-2)}\|_{\infty} = \max_{1 \leq j \leq m} |\psi_{\text{sc}}^{(k-2)}(\mathbf{r}_j)| = \|\psi_{\text{sc}}^{(k-2)}\|_{\infty}.$$

Combining (3.7)–(3.11) yields

$$(3.12) \quad \|\psi_{\text{sc}}^{(k)}\|_{\infty} \leq C\sigma_{\text{max}} \|\psi_{\text{sc}}^{(k-2)}\|_{\infty},$$

where $C = \prod_{i=1}^4 C_i$. We have from the same argument that the infinite series for $\psi_{\text{sc}}^{(k)}$ is convergent when the maximum magnitude of the scattering coefficients σ_{max} is small enough.

3.2. Far-field patterns. Of particular interest in scattering theory are the far-field patterns, or scattering amplitudes, of the scattered waves. The far-field patterns of scattering waves for time-harmonic incident waves play a fundamental role in the inverse scattering theory due to the fact that they induce the important geometrical and physical information, e.g., the location, shape, and impedance of the boundary,

on the scattering object. This section investigates the convergence of the far-field patterns.

More specifically, given an incident field with incident direction \mathbf{d} , if u_{sc} is the scattered field, then u_{sc} has the asymptotic behavior

$$(3.13) \quad u_{sc} = \frac{e^{i\kappa|\mathbf{r}|}}{|\mathbf{r}|} [u_\infty(\hat{\mathbf{r}}) + O(|\mathbf{r}|^{-1})] \quad \text{as } |\mathbf{r}| \rightarrow \infty$$

uniformly in all directions $\hat{\mathbf{r}} = \mathbf{r}/|\mathbf{r}|$, where the function u_∞ , defined on the unit sphere, is called as the far-field pattern of u_{sc} and $\hat{\mathbf{r}}$ is known as the observation direction.

We next derive the far-field patterns for the m point scatterers and the extended obstacle scatterer separately, followed by the far-field pattern for the multiple scattering problem involving both the point scatterers and the extended obstacle.

Recall for large arguments we have the following asymptotic behavior for Green's function:

$$\frac{e^{i\kappa|\mathbf{r}-\mathbf{r}'|}}{|\mathbf{r}-\mathbf{r}'|} = \frac{e^{i\kappa|\mathbf{r}|}}{|\mathbf{r}|} [e^{-i\kappa\hat{\mathbf{r}}\cdot\mathbf{r}'} + O(|\mathbf{r}|^{-1})] \quad \text{as } |\mathbf{r}| \rightarrow \infty.$$

Comparing with (3.13), we obtain from (2.6) and the following identity

$$|\mathbf{r}-\mathbf{r}'| = \sqrt{|\mathbf{r}|^2 - 2\mathbf{r}\cdot\mathbf{r}' + |\mathbf{r}'|^2} = |\mathbf{r}| - \hat{\mathbf{r}}\cdot\mathbf{r}' + O(|\mathbf{r}|^{-1}) \quad \text{as } |\mathbf{r}| \rightarrow \infty$$

that the far-field pattern of the scattered field for the m point scatterers is

$$(3.14) \quad u_{\infty,p}(\hat{\mathbf{r}}) = \frac{1}{4\pi} \sum_{j=1}^m A_j e^{-i\kappa\hat{\mathbf{r}}\cdot\mathbf{r}_j}.$$

It follows from the integral representation of the scattered field (2.12) and the asymptotic expansion of Green's function that the far-field pattern for the obstacle is given by

$$(3.15) \quad u_{\infty,o}(\hat{\mathbf{r}}) = -\frac{1}{4\pi} \int_{\Gamma} \partial_{\mathbf{n}'} u(\mathbf{r}') e^{-i\kappa\hat{\mathbf{r}}\cdot\mathbf{r}'} ds(\mathbf{r}').$$

Define the far-field pattern for the multiple scattering problem as

$$(3.16) \quad u_\infty(\hat{\mathbf{r}}) = u_{\infty,p}(\hat{\mathbf{r}}) + u_{\infty,o}(\hat{\mathbf{r}}),$$

where the far-field pattern, $u_{\infty,p}$, due to the point scatterers, is

$$(3.17) \quad u_{\infty,p}(\hat{\mathbf{r}}) = \sum_{k=1}^{\infty} u_{\infty,p}^{(k)}(\hat{\mathbf{r}}) = \frac{1}{4\pi} \sum_{j=1}^m e^{-i\kappa\hat{\mathbf{r}}\cdot\mathbf{r}_j} \sum_{k=1}^{\infty} A_j^{(k)},$$

and the far-field pattern, $u_{\infty,o}$, due to the extended obstacle, is

$$(3.18) \quad u_{\infty,o}(\hat{\mathbf{r}}) = \sum_{k=1}^{\infty} u_{\infty,o}^{(k)}(\hat{\mathbf{r}}) = -\frac{1}{4\pi} \int_{\Gamma} e^{-i\kappa\hat{\mathbf{r}}\cdot\mathbf{r}'} \sum_{k=1}^{\infty} \partial_{\mathbf{n}'} \psi^{(k)}(\mathbf{r}') ds(\mathbf{r}').$$

Next we consider the convergence for the far-field patterns $u_{\infty,p}$ and $u_{\infty,o}$ separately. Taking magnitudes on both sides of (3.16) and using the definition for the maximum norm of a vector yields

$$(3.19) \quad |u_{\infty,p}(\hat{\mathbf{r}})| \leq \frac{1}{4\pi} \sum_{m=1}^{\infty} \|A^{(m)}\|_{\infty}.$$

To prove the convergence of the infinite series for $u_{\infty,p}$ in (3.16), it suffices to prove the convergence of the infinite series in the right-hand side of (3.18). We will briefly outline the following estimates since they are basically the same as those in the proof for the scattered fields given in the previous subsection.

It follows from Theorem 2.1 that

$$(3.20) \quad \| A^{(k)} \|_{\infty} \leq C_2 \sigma_{\max} \| \phi_{\text{sou}}^{(k-1)} \|_{\infty} .$$

We have from the definition of the source field (2.21) and the integral representation (2.18) that

$$(3.21) \quad \| \phi_{\text{sou}}^{(k-1)} \|_{\infty} \leq C_3 \| \partial_{\mathbf{n}} \psi^{(k-1)} \|_{0,\infty,\partial D} .$$

Applying Theorem 2.2 leads to

$$(3.22) \quad \| \partial_{\mathbf{n}} \psi^{(k-1)} \|_{0,\infty,\Gamma} \leq C_4 \| \phi_{\text{sc}}^{(k-2)} \|_{1,\infty,\Gamma} .$$

We get from (2.17) that

$$(3.23) \quad \| \phi_{\text{sc}}^{(k-2)} \|_{1,\infty,\Gamma} \leq C_1 \| A^{(k-2)} \|_{\infty} .$$

Combining (3.20)–(3.23) yields

$$(3.24) \quad \| A^{(k)} \|_{\infty} \leq C \sigma_{\max} \| A^{(k-2)} \|_{\infty} .$$

The proof is done when σ_{\max} is assumed to be small enough.

Next we consider the convergence for the far-field patterns $u_{\infty,o}$. Evidently, we have

$$(3.25) \quad |u_{\infty,o}(\hat{\mathbf{r}})| \leq \frac{|\Gamma|}{4\pi} \sum_{k=1}^{\infty} \| \partial_{\mathbf{n}} \psi^{(k)} \|_{0,\infty,\Gamma} .$$

The convergence of the dominated infinite series can be verified as σ_{\max} is small enough by the following estimates:

$$(3.26) \quad \| \partial_{\mathbf{n}} \psi^{(k)} \|_{0,\infty,\Gamma} \leq C \sigma_{\max} \| \partial_{\mathbf{n}} \psi^{(k-2)} \|_{0,\infty,\Gamma} .$$

In the proof of the convergence for the scattered fields and the far-field pattern, the maximum magnitude of the scattering coefficient σ_{\max} is assumed to be small enough to guarantee the dominated infinite series are geometrical series. When σ_{\max} is small, the scattered field from the point scatterers can be regarded as a small perturbation to the scattered field from the extended obstacle. Therefore, the obstacle consisting of small scale scatterers can be treated as a small perturbation to the extended obstacle. In a practical situation, it will make sense since interested obstacles are usually embedded in a small scale cluttered medium instead of idealized free space.

Remark 3.1. Based on the integral equation formulation (2.23) for the multiple scattering problem and the asymptotic behavior for Green’s function, we may also obtain the far-field pattern of the scattered field

$$(3.27) \quad u_{\infty}(\hat{\mathbf{r}}) = \frac{1}{4\pi} \sum_{j=1}^m \sigma_j u_j e^{-i\kappa \hat{\mathbf{r}} \cdot \mathbf{r}_j} - \frac{1}{4\pi} \int_{\Gamma} \partial_{\mathbf{n}'} u(\mathbf{r}') e^{-i\kappa \hat{\mathbf{r}} \cdot \mathbf{r}'} ds(\mathbf{r}').$$

The far-field pattern (3.27) will be computed as a comparison with the far-field pattern (3.16)–(3.18) based on the series solution formulation.



FIG. 3. Test cases, obstacle surfaces: (left) smooth surface of a unit sphere; (right) rough surface of a distorted unit sphere.

4. Numerical experiments. In this section, we discuss computational aspects of the boundary element method, present some examples to illustrate the performance of the proposed method, and show the features of the far-field patterns for the scattered fields in the multiple scattering problem.

The Galerkin boundary element method is chosen to solve the boundary integral equations. For other numerical methods, the reader is referred to Bates and Wall [1] for the null field approach, to Waterman [15, 16] for the extended boundary condition method, and to Peterson and Ström [12] for the T-matrix method. See also Chew [3] for recent accounts of the numerical methods to the obstacle scattering problem. In the implementation of the boundary integral equations, singular integrals have to be evaluated. We decompose the singular integrals into two parts: the first part is the entry of the double layer potential matrix corresponding to the Laplace operator, while the remaining part has no singularity for $\mathbf{r} \rightarrow \mathbf{r}'$. The first part can be analytically evaluated, and the remaining part can be computed numerically, such as an adaptive Gaussian quadrature rule for each triangle. We refer to [13] for detailed descriptions on the evaluation of singular integrals arising from the Galerkin boundary element method for solving boundary integral equations. As for the linear solver, we use the direct method of LU decomposition with partial pivoting, which is efficient for the series solution formulation since the matrices are decomposed once and can be used in all iterations.

Figure 3 shows typical meshes for the test cases of the obstacle surfaces considered: the smooth surface of a unit sphere and the rough surface of a distorted sphere. The surfaces are triangulated using the maximal speed molecular surface (MSMS) package of Sanner and Olson [14]. Two types of distribution of the point scatterers are considered: uniformly distributed point scatterers and randomly distributed point scatterers. In the following two examples, the wavenumber κ is taken as π , i.e., the wavelength of the incident field is $\lambda = 2$. The far-field patterns will be plotted on the unit sphere as a function of the variables for the latitudinal angle and the longitudinal varying from 0 to π and from 0 to 2π , respectively. All the figures are shown from the view corresponding to the observation direction $(0, 0, 1)^\top$.

Example 1. Consider a heterogeneous medium consisting of ten uniformly distributed point scatterers and a smooth surface of the unit sphere. The ten uniformly distributed point scatterers are at $\mathbf{r}_j = 2(\cos(j\pi/2), \sin(j\pi/2), 0)^\top$, $j = 0, \dots, 9$. In this example, the scattering coefficients for the ten point scatterers are equally taken as the unit. Figures 4 and 5 show the real and imaginary parts of the far-field patterns for the scattered fields with incident direction $\mathbf{d} = (1, 0, 0)^\top$ and $\mathbf{d} = (0, 0, 1)^\top$, respectively. It is meant to be representative to present the results using these two incident directions since the results are similar with other directions. In each figure, the top row shows the real part (left) and the imaginary part (right) of the far-field

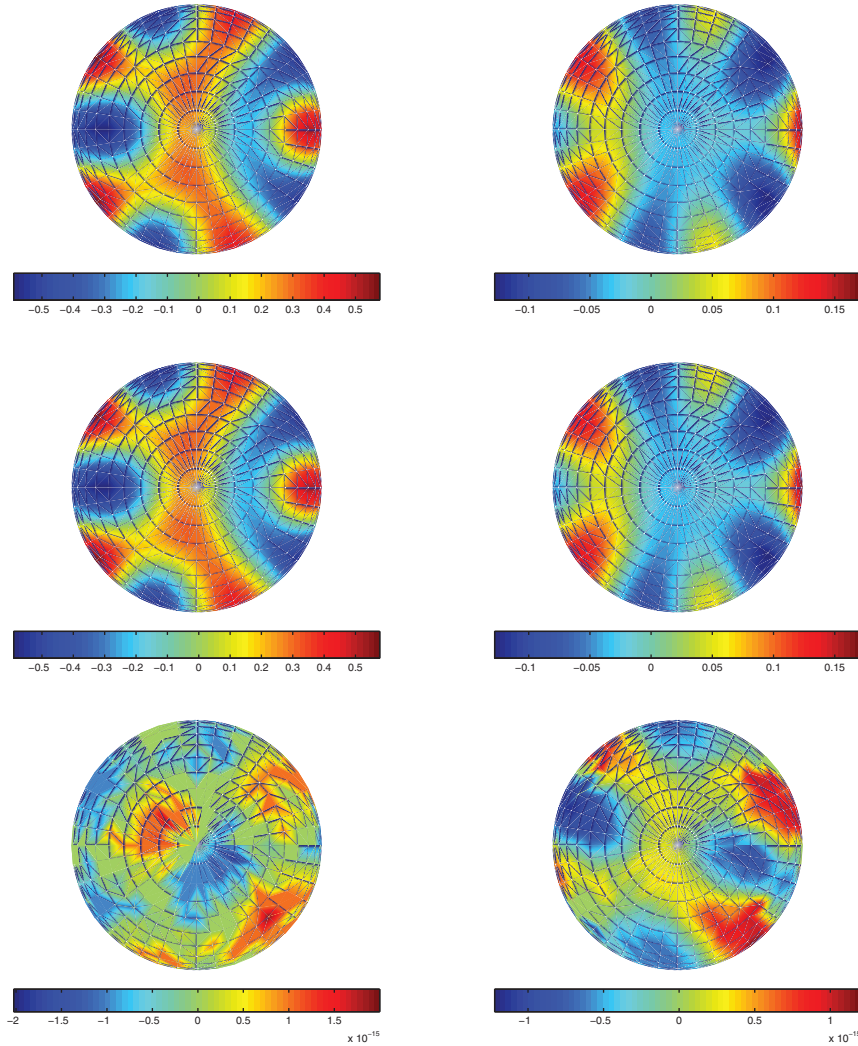


FIG. 4. The far-field pattern of the scattered field for Example 1 with the incident direction $\mathbf{d} = (1, 0, 0)^T$. (Top row) The real and imaginary parts of the far-field pattern computed from the integral equation formulation; (middle row) the real and imaginary parts of the far-field pattern computed from the series solution formulation; (bottom row) the error for the real and imaginary parts of the far-field pattern between two formulations.

pattern computed from the integral equation formulation; the middle row plots the real and imaginary parts of the far-field pattern computed from the series solution formulation; the bottom row displays the error of the real and imaginary parts of the far-field patterns from the two different formulations. As can be seen from the figures, the error is at the level of the machine accuracy. The two formulations perfectly match and the solution from the series formulation converges well to the solution from the integral equation formulation. In order to show whether proposed methods numerically capture the multiple scattering between the extended obstacle and the point scatterers, Figures 6 and 7 plot the difference of the far-field patterns corresponding to the extended obstacle in the presence of point scatterers against the same obsta-

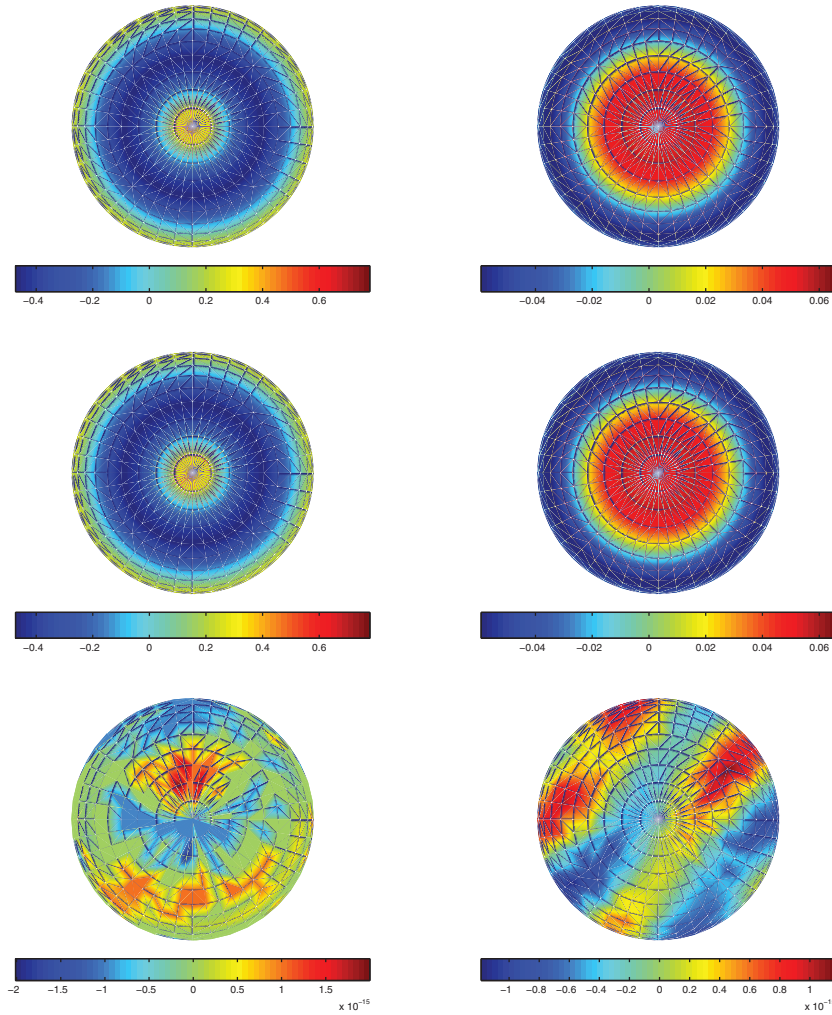


FIG. 5. The far-field pattern of the scattered field for Example 1 with the incident direction $\mathbf{d} = (0, 0, 1)^\top$. (Top row) The real and imaginary parts of the far-field pattern computed from the integral equation formulation; (middle row) the real and imaginary parts of the far-field pattern computed from the series solution formulation; (bottom row) the error for the real and imaginary parts of the far-field pattern between two formulations.

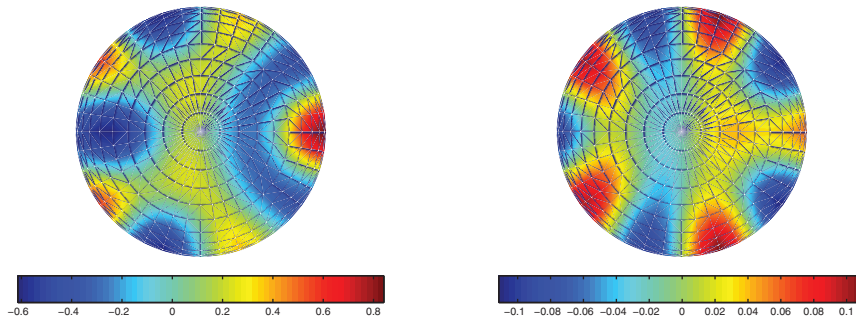


FIG. 6. Example 1. The difference of the far-field patterns in the presence of point scatterers against the absence of point scatterers corresponding to the incident direction $\mathbf{d} = (1, 0, 0)^\top$. (Left) The real part; (right) the imaginary part.

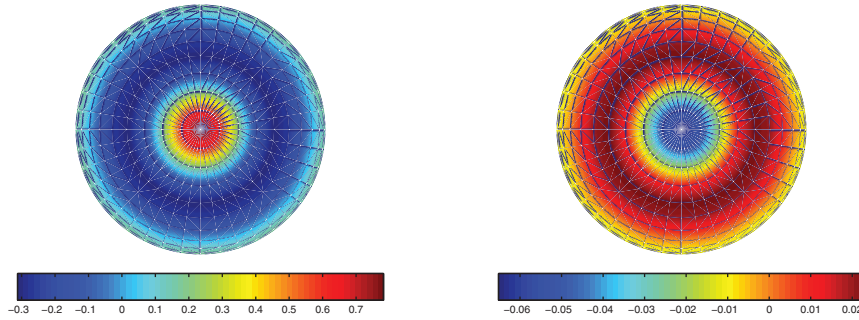


FIG. 7. *Example 1. The difference of the far-field patterns in the presence of point scatterers against the absence of point scatterers corresponding to the incident direction $\mathbf{d} = (0, 0, 1)^\top$. (Left) The real part; (right) the imaginary part.*

cle in the absence of point scatterers for the incident directions $\mathbf{d} = (1, 0, 0)^\top$ and $\mathbf{d} = (0, 0, 1)^\top$, respectively.

Example 2. Consider a heterogeneous medium consisting of 100 randomly distributed point scatterers and the rough surface of a distorted sphere. This example mimics the practical situation when a complicated obstacle is immersed in a cluttered medium with randomly distributed small scale scatterers. The 100 point scatterers are randomly distributed in the annulus region between two spheres with radii 2 and 3. The scattering coefficients are uniformly distributed random numbers ranging from 0 to 1. As is similar to the previous example, Figures 8 and 9 show the real and imaginary parts of the far-field patterns for the scattered fields with incident direction $\mathbf{d} = (1, 0, 0)^\top$ and $\mathbf{d} = (0, 0, 1)^\top$, respectively. In each figure, the top row shows the real part (left) and the imaginary part (right) of the far-field pattern computed from the integral equation formulation; the middle row plots the real and imaginary parts of the far-field pattern computed from the series solution formulation; the bottom row displays the error of the real and imaginary parts of the far-field patterns from the two different formulations. Seen from the error level, the agreement of the solutions from two approaches is obtained. Again, Figures 10 and 11 plot the difference of the far-field patterns corresponding to the extended obstacle in the presence of point scatterers against the same obstacle in the absence of point scatterers for the incident directions $\mathbf{d} = (1, 0, 0)^\top$ and $\mathbf{d} = (0, 0, 1)^\top$, respectively.

5. Conclusion. We developed a generalized Foldy–Lax method for the two-scale multiple acoustic wave scattering problem in a heterogeneous medium consisting of point scatterers and an extended obstacle in three-dimensional space. Two formulations are presented: one is based on the series solution formulation, and another is based on an integral equation formulation. The method combined the Foldy–Lax self-consistent method with the boundary integral method for computing the scattered fields from the point scatterers and the extended obstacle. It takes full account of the multiple scattering among the point scatterers and between the point scatterers and the extended obstacle. Computationally, the series solution formulation describes an iterative procedure, and orders of scattering can be evaluated efficiently at each step. Since the coefficient matrices for the point scatterers and the extended obstacle do not change in iterations, LU decomposition with partial pivoting needs to occur only once at the beginning, and the decomposed matrices can be used in all iterations. We verified the geometrical property of the infinity series and proved the convergence of the scattered fields and the far-field patterns when the scattering coefficients are

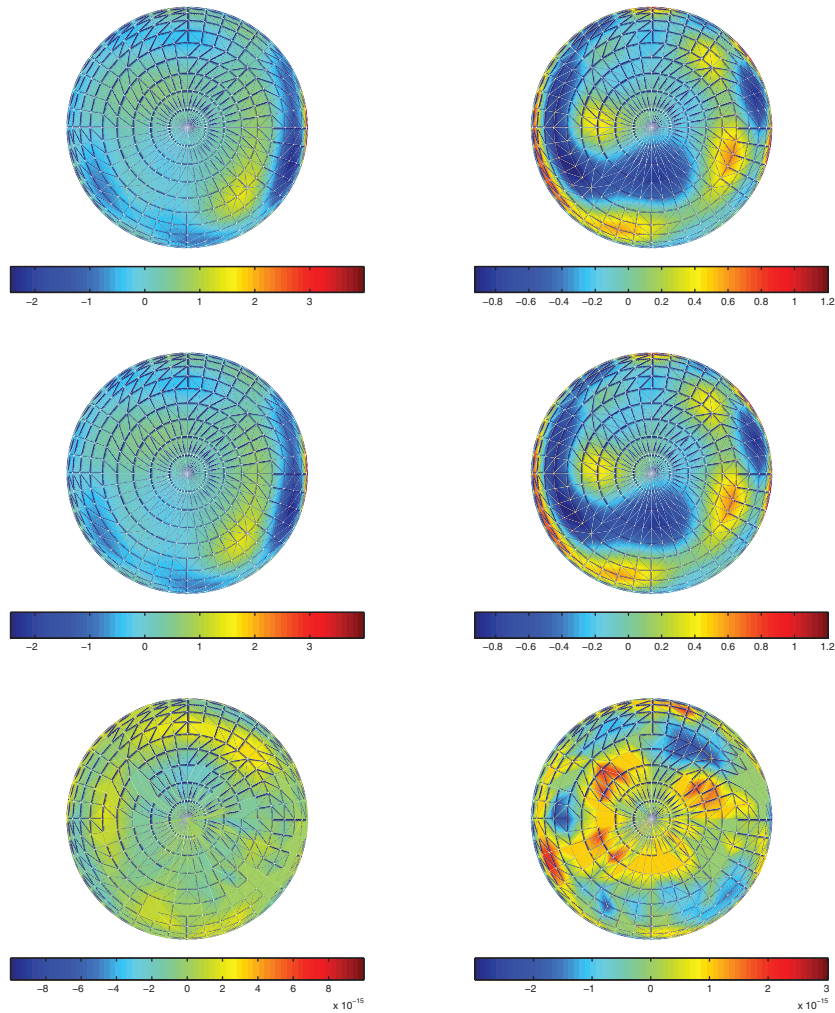


FIG. 8. The far-field pattern of the scattered field for Example 2 with the incident direction $\mathbf{d} = (1, 0, 0)^T$. (Top row) The real and imaginary parts of the far-field pattern computed from the integral equation formulation; (middle row) the real and imaginary parts of the far-field pattern computed from the series solution formulation; (bottom row) the error for the real and imaginary parts of the far-field pattern between two formulations.

small. Numerical examples were presented, with uniformly and randomly distributed point scatterers and with obstacles with smooth and rough surfaces. The far-field patterns and the convergence of the series solution formulation were reported, and the results show the good agreement of the proposed two formulations.

We intend to apply the proposed method to solve the inverse obstacle scattering problems, where the obstacles are embedded in a cluttered environment with many small scale point scatterers. The direct applications will be in time-reversal imaging and near-field optical microscopy [6], which provide feasible approaches to super-resolution. We also plan to modify the Foldy–Lax method and to extend the method for multiscale multiple electromagnetic wave scattering problems, which involves three-dimensional Maxwell’s equations and vector fields.

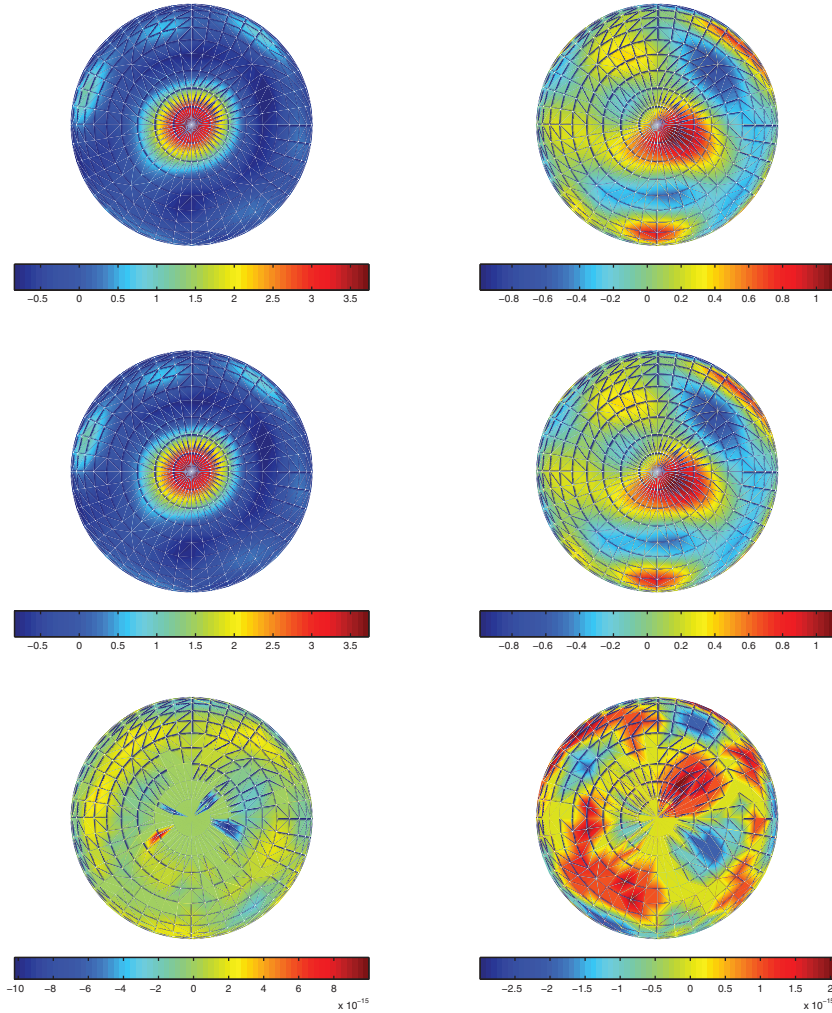


FIG. 9. The far-field pattern of the scattered field for Example 2 with the incident direction $\mathbf{d} = (0, 0, 1)^\top$. (Top row) The real and imaginary parts of the far-field pattern computed from the integral equation formulation; (middle row) the real and imaginary parts of the far-field pattern computed from the series solution formulation; (bottom row) the error for the real and imaginary parts of the far-field pattern between two formulations.

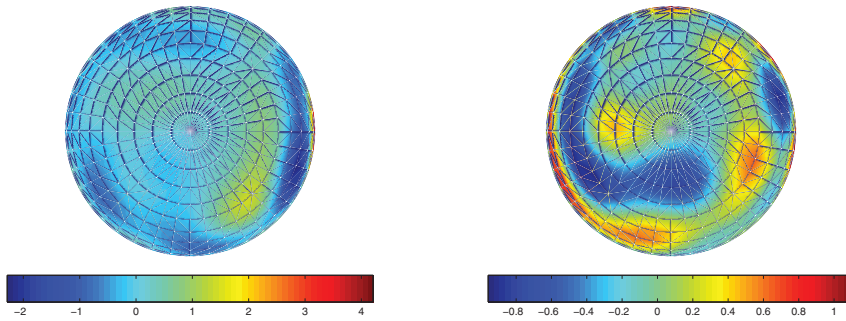


FIG. 10. Example 2. The difference of the far-field patterns in the presence of point scatterers against the absence of point scatterers corresponding to the incident direction $\mathbf{d} = (1, 0, 0)^\top$. (Left) The real part; (right) the imaginary part.

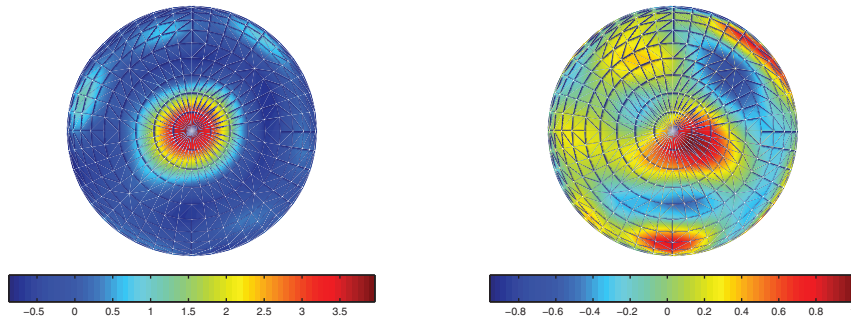


FIG. 11. *Example 2. The difference of the far-field patterns in the presence of point scatterers against the absence of point scatterers corresponding to the incident direction $\mathbf{d} = (0, 0, 1)^\top$. (Left) The real part; (right) the imaginary part.*

Acknowledgments. We wish to thank the reviewers for their helpful comments to improve the manuscript.

REFERENCES

- [1] R. BATES AND D. WALL, *Null field approach to scalar diffraction, I. General methods, II. Approximation method*, Philos. Trans. R. Soc. Lond. Ser. A Math. Phys. Eng. Sci., 287 (1977), pp. 45–95.
- [2] H. BRAKHAGE AND P. WERNER, *Über das Dirichletsche Aussenraum Problem für die Helmholtzsche Schwingungsgleichung*, Arch. Math. (Basel), 16 (1965), pp. 325–329.
- [3] W. C. CHEW, *Waves and Fields in Inhomogeneous Media*, Van Nostrand Reinhold, New York, 1990.
- [4] D. COLTON AND R. KRESS, *Inverse Acoustic and Electromagnetic Scattering Theory*, Appl. Math. Sci. 93, Springer, Berlin, 1998.
- [5] D. COLTON AND R. KRESS, *Integral Equation Methods in Scattering Theory*, Pure Appl. Math., John Wiley, New York, 1983.
- [6] D. COURJON, *Near-field Microscopy and Near-field Optics*, Imperial College Press, London, 2003.
- [7] L. FOLDY, *The multiple scattering of waves. I. General theory of isotropic scattering by randomly distributed scatterers*, Phys. Rev., 67 (1945), pp. 107–119.
- [8] K. HUANG, K. SOLNA, AND H. ZHAO, *Generalized Foldy–Lax formulation*, J. Comput. Phys., 229 (2010), pp. 4544–4553.
- [9] R. KRESS, *Minimizing the condition number of boundary integral operators in acoustic and electromagnetic scattering*, Quart. Mech. Appl. Math., 38 (1985), pp. 323–341.
- [10] M. LAX, *Multiple scattering of waves*, Rev. Modern Phys., 23 (1951), pp. 287–310.
- [11] P. MARTIN, *Multiple Scattering: Interaction of Time-Harmonic Wave with N Obstacles*, Encyclopedia Math. Appl. 107, Cambridge University Press, Cambridge, 2006.
- [12] B. PETERSON AND S. STRÖM, *T matrix for electromagnetic scattering from an arbitrary number of scatterers and representations of $E(3)$* , Phys. Rev. D, 8 (1973), pp. 3661–3678.
- [13] S. RJASANOW AND O. STEINBACH, *The Fast Solution of Boundary Integral Equations*, Springer, New York, 2007.
- [14] M. SANNER AND A. OLSON, *Reduced surface: An efficient way to compute molecular surfaces*, Biopolymers, 38 (1996), pp. 305–320.
- [15] P. WATERMAN, *New formulation of acoustic scattering*, J. Acoust. Soc. Am., 45 (1969), pp. 1417–1429.
- [16] P. WATERMAN, *Symmetry, unitarity and geometry in electromagnetic scattering*, Phys. Rev. D, 3 (1971), pp. 825–829.